IOP Conf. Series: Materials Science and Engineering **433** (2018) 012054 doi:10.1088/1757-899X/433/1/012054

Turbulent Forced Convection of Nanofluids Flow in Corrugated Tubes

Abdalrazzaq K. Abbas and Nabeel S. Dhaidan[a]
[a] Corresponding author; E-mail address: engnab74@yahoo.com.

Department of Mechanical Engineering, College of Engineering, University of Kerbala, Kerbala, Iraq

Abstract. The heat transfer enhancement and accompanied pressure drop penalty caused by using nanofluids as the heat transfer fluids in corrugated tubes was investigated numerically. The study involved the dispersion of SiO_2 nanoparticles at different concentrations and sizes in the base fluid at various Reynolds numbers from 5,000 to 60,000. The simulation adopted a k-ε model and FLUENT-based control volume to solve the turbulent flow field and associated thermal behaviours of the nanofluids. The volume fraction of nanoparticles varied from 1% to 4%, while the size of the nanoparticles ranged from 30 nm to 80 nm in diameter. The thermal and hydrodynamic performance of nanofluids were compared with those of the base fluid, and the calculated results were validated by, and agree well with, the findings of previous work. The simulated results reveal that the heat exchange rate is greatly influenced by the use of different nanofluids parameters. Enhancements in the rate of heat transfer and expanse of pressure drop and resultant pumping energy are associated with the dispersion of more nanoparticles and/or a decrease in the nanoparticle size. Moreover, it was found that the effect of nanoparticle loading is more significant than the effect of nanoparticle size. Further, the techniques of heat transfer (corrugation and nanoparticles) were found to be ineffective for Reynolds numbers greater than 40,000.

Keywords

Nanofluids, turbulent forced convection, flow through corrugated tube, heat transfer enhancement

Nomenclature

C_p	Specific heat, kJ kg^{-1} K^{-1}
d	Tube inside diameter, m
d_h	Hydraulic diameter, m
d_p	Nanoparticles diameter, nm
e	Roughness height, m
E	Total energy, J
f	Darcy friction factor

Content from this work may be used under the terms of the Creative Commons Attribution 3.0 licence. Any further distribution of this work must maintain attribution to the author(s) and the title of the work, journal citation and DOI.
Published under licence by IOP Publishing Ltd

G_k	Generation of turbulent kinetic energy due to mean velocity gradients
kt	Thermal conductivity, W $m^{-1} K^{-1}$
k	Turbulent kinetic energy, J kg^{-1}
L	Length of tube entrance, m
Nu	Average Nusselt number
P	Pressure, N m^{-2}
p	Pitch of corrugated, m
PEC	Performance evaluation criteria
Pr	Prandtl number
ΔP	Pressure drop, P_{inlet} -P_{outlet}, N m^{-2}
q''	Heat flux rate applied on the tube wall, W m^{-2}
r	Redial-direction
Re	Reynolds number
T	Temperature, K
T_b	Bulk temperature, K
T_w	Wall temperature, K
u	Flow velocity component, m s^{-1}
u_m	Mean velocity of flow, m s^{-1}
u'	Fluctuated velocity (local flow velocity), m s^{-1}
w	Width of corrugated, m
x	Axis-direction

Greek Symbols

ρ	Density of fluid, kg m^{-3}
μ	Dynamic viscosity, N s m^{-2}
ε	Turbulent dissipation rate, m^2 s^{-3}
ϕ	Nanoparticles volume fraction
τ	Shear stress, kg m^{-2}
σ_ε	Effective Prandtl numbers for turbulent rate of dissipation
σ_k	Effective Prandtl numbers for turbulent kinetic energy

Subscripts

bf	Base fluid
nf	Nanofluid
p	Particle
w	Wall
t	Turbulent

1. Introduction

Conventional heat transfer fluids suffer from low thermal conductivity, which suppresses the heat transfer rate in heating and cooling applications. Three methods can be utilised to enhance the heat transfer rate: active, passive, and compound. Active methods require external power to augment heat transfer, and include mechanical aids, surface and/or fluid vibration, and electrohydrodynamic techniques. Passive techniques rely on exciting turbulence near the tube wall surface to minimise growth by means of static techniques such as fins, spirally roughened tubes, ribbed tubes, corrugated tubes, and helical tubes. Compound heat transfer enhancement methods employ both active and passive techniques simultaneously. A modern technique for heat transfer enhancement in fluids involves the use of nanofluids, which are composed of dispersions of conductive solid nanoparticles in a base fluid [1], which cause the effective thermal conductivity to increase, further enhancing heat transfer.

Darzi et al. [2] experimentally investigated the influence of various volume loadings of SiO_2-water nanofluids (≤ 1 vol%) on the thermal and hydrodynamic performance of turbulent flow inside various heights and pitches of helically corrugated tube. It was concluded that decreasing the pitch of corrugation and decreasing the corrugated height enhanced the heat transfer, and that using a specified loading of nanoparticles augmented the heat exchange with only a small penalty in the form of pressure drop. Manca et al. [3] numerically investigated the flow field and heat transfer of Al_2O_3-water nanofluids (≤ 4 vol%) of various nanoparticle concentrations inside ribbed channels of rectangular and square shape using a single-phase approach. It is inferred that the observed augmentation in the rate of heat exchange and drop in pressure was achieved due to the introduction of the nanoparticles. Darzi et al. [4] applied a two-phase model to numerically investigate the thermal and hydraulic performance of the flow of Al_2O_3–water nanofluids (≤ 4 vol%) inside helically corrugated tubes. The effects of the pitch and height of corrugation, nanoparticle volume fraction and the Reynolds number were considered. The enhancements in heat transfer were 21% and 58% utilising nanofluids of 2 vol% and 4 vol %, respectively, compared with using water. Later, Darzi et al. [5] conducted experiments to investigate the heat transfer and friction factor of flow of Al_2O_3-water nanofluids (≤ 1 vol%) through a helical-corrugated tube. The maximum augmentation in the rate of heat exchange was about 320% for a higher loading of nanoparticles, and a small pitch and higher height of corrugation. Here, the effect of corrugation was seen to be more significant for enhancement than adding nanoparticles. A computational study to investigate the forced convection flow of nanofluids (≤ 4 vol%) inside channels with different rib-groove shapes was performed by Al-Shamani et al. [6]. The controlled parameters considered in the study were nanoparticles types (*CuO*, Al_2O_3, *ZnO*, and SiO_2), sizes of nanoparticles, and nanoparticle volume loadings. It was inferred that the SiO_2-water nanofluids had the highest rate of heat transfer and that the maximum Nusselt number was achieved for the trapezoidal rib-groove channel.

An experimental and numerical study to investigate the thermal enhancement and pressure drop penalty produced by employing Al_2O_3-water nanofluids (≤ 3 vol%) inside corrugated tubes of different rib dimensions was conducted by Khdher et al. [7]. The results revealed that the enhancements in the Nusselt number and friction factor depended on the nanoparticle volume loading, rib geometry, and operating conditions. Navaei et al. [8] numerically studied the 2D turbulent forced convection flow of nanofluids (≤ 4 vol.%) inside ribbed tubes with different rib-shapes and sizes, using various base-fluids, and different nanoparticle loadings and diameters. It was concluded that the Nusselt number was enhanced by increased loading of nanoparticles and decreased as the diameter of nanoparticles increased. In contrast, the friction factor varied insignificantly with the loading and diameter of nanoparticles. Yang et al. [9] conducted an experimental study to examine the thermal and flow behavior of MWCNT-R141b nano-refrigerant (≤ 0.3 wt%) flowiing in a corrugated tube. It was found that adding nanoparticles to refrigerants enhanced the heat transfer, but also caused an increase in pumping power at the same time. Andreozzi et al. [10] performed a numerical study to analyse the forced convection turbulent flow of Al_2O_3-water nanofluids (≤ 4 vol.%) through ribbed channels of rectangular, trapezoidal, and triangular rib-shapes. It was found that increasing the number of nanoparticles led to an augmentation of the Nusselt number and increased the required pumping power. Triangular-ribbed channels achieved higher thermal performance and higher-pressure loss compared with trapezoidal-ribbed ones. Kumar et al. [11] performed an experimental and numerical investigation of thermal characteristics of nanofluids (≤ 4 vol%) of different nanoparticles (Al_2O_3, *ZnO,* and *CuO*) inside a square channel with protruding ribs. The results revealed that the thermal exchange of nanofluids was enhanced as the nanoparticle diameter decreased and nanoparticle concentration increased, and that Al_2O_3-water nanofluids had the highest Nusselt number. Qi et al. [12] conducted experiments and a numerical investigation to examine the heat exchange augmentation and pressure drop of TiO_2-water nanofluids (≤ 0.5 wt%) in corrugated tubes. It was shown that the heat transfer associated with the flow of nanofluids inside corrugated tubes can be enhanced by 53.95% compared with the base fluid flows inside a smooth tube. At the same Reynolds number, the maximum difference in friction factor was found to be less than 4% between the nanofluids and base fluid.

In this research, a numerical investigation of the thermal and hydrodynamic behaviours of nanofluids (SiO_2-water) inside corrugated tubes will be carried out for a high range of Reynolds numbers (5,000 to 60,000). The effect of the size and volumetric concentrations of nanoparticles on the heat transfer as well as the friction factor of the nanofluids will also be examined. Performance evaluation criteria will also be examined to assess two enhancement techniques: corrugation and nanoparticle dispersion.

2. Problem Formulation

A schematic representation of the fully developed flow of SiO_2-water nanofluids (ϕ=1 to 4 vol.% and d_p=30 to 80 nm) inside a corrugated tube of 10 mm diameter is depicted in figure 1. The A constant heat flux of 50 W/m^2 is assumed to be uniformly presented to the external wall of the tube. The corrugation of the tube is represented by the rib pitch of 5 mm, the rib height of 0.25 mm, and the rib width of 2 mm. The flow through the straight, rough, circular tube is assumed to be steady, incompressible, two-dimensional, and Newtonian, and radiation, dissipation, and end effects are negligible. No slip conditions and no temperature difference between the base fluid and the nanoparticles are taken into consideration. A single-phase model is thus applied to calculate the

effective thermophysical properties of nanofluids from the properties of their components, which are listed in Table 1.

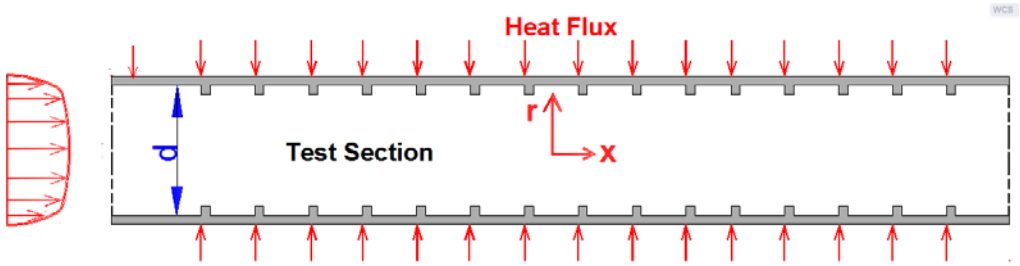

Figure 1. Schematic representation of the model.

Table 1. Thermophysical properties of water and SiO_2-nanoparticles.

Thermophysical Properties	Water	SiO_2-nanoparticles
Density, ρ (kg/m^3)	996.5	2220
Specific heat, C_p (J/kg.K)	4181	745
Thermal conductivity, *kt* (W/m.K)	0.6103	1.4
Dynamic Viscosity, μ (N.s/m^2)	0.00100	-

The hydrodynamic-thermal behaviour of the flow is modelled by applying continuity, momentum, and energy equations as in equations 1, 2, and 3, respectively.

$$\frac{\partial u_i}{\partial x_i} = 0 \tag{1}$$

$$\frac{\partial}{\partial x_i}(\rho_{nf}\, u_i\, u_j) = -\frac{\partial P}{\partial x_i} + \frac{\partial}{\partial x_j}\left[\mu_{nf}\left(\frac{\partial u_i}{\partial x_j} + \frac{\partial u_j}{\partial x_i} - \frac{2}{3}\delta_{ij}\frac{\partial u_i}{\partial x_j}\right)\right] + \frac{\partial}{\partial x_i}(-\rho_{nf}\,\overline{u_i' u_j'}) \tag{2}$$

$$\frac{\partial}{\partial x_i}\left[u_i(\rho_{nf}\, E + P)\right] = \frac{\partial}{\partial x_j}\left[\frac{\partial T}{\partial x_j}\left(kt_{nf} + \frac{C_{p,nf}\,\mu_t}{\mathrm{Pr}_t}\right) + u_i(\tau_{ij})_{eff}\right] \tag{3}$$

The deviatoric stress tensor is defined as

$$(\tau_{ij})_{eff} = \mu_{nf}\left(\frac{\partial u_i}{\partial x_j} + \frac{\partial u_j}{\partial x_i}\right) - \frac{2}{3}\mu_{nf}\frac{\partial u_i}{\partial x_j}\delta_{ij} \tag{4}$$

A *k-ε* turbulent model was thus applied. The rate of dissipation (ε) and turbulent kinetic energy (k) are evaluated as

$$\frac{\partial}{\partial x_i}(\rho_{nf}\, k\, u_i) = \frac{\partial}{\partial x_j}\left[(\mu_{nf} + \frac{\mu_t}{\sigma_k})\frac{\partial k}{\partial x_j}\right] + G_k - \rho_{nf}\,\varepsilon \tag{5}$$

$$\frac{\partial}{\partial x_i}(\rho_{nf}\,\varepsilon\,u_i)=\frac{\partial}{\partial x_j}[(\mu_{nf}+\frac{\mu_t}{\sigma_\varepsilon})\frac{\partial \varepsilon}{\partial x_j}]+C_{1\varepsilon}(\varepsilon/k)G_k-C_{2\varepsilon}\,\rho_{nf}(\varepsilon^2/k) \quad (6)$$

The eddy viscosity, μ_t, is expressed as:

$$\mu_t=\frac{\rho_{nf}\,C_\mu\,k^2}{\varepsilon} \quad (7)$$

Where $\sigma_k=1.0$, $\sigma_\varepsilon=1.3$ $C_\mu=0.09$, $C_{1\varepsilon}=1.44$ and $C_{2\varepsilon}=1.92$,.

The effective thermophysical properties of nanofluids, density, heat capacitance, thermal conductivity, and viscosity, are estimated by Equations 8 to 11, respectively.

$$\rho_{nf}=(1-\phi)\,\rho_{bf}+\phi\,\rho_p \quad (8)$$

$$(\rho\,C_p)_{nf}=(1-\phi)(\rho\,C_p)_{bf}+\phi(\rho\,C_p)_p \quad (9)$$

$$\frac{kt_{nf}}{kt_{bf}}=\frac{kt_p+2kt_{bf}-2\phi(kt_f-kt_p)}{kt_p+2kt_{bf}+\phi(kt_f-kt_p)} \quad (10)$$

$$\mu_{nf}=\mu_{bf}\,(123\,\phi^2+7.3\,\phi+1) \quad (11)$$

The flow and thermal behaviours are characterised by their dimensionless parameters, the average Nusselt numbers, the Reynolds number, and the Darcy friction factor, which are calculated respectively as

$$Nu=\frac{q^{"}\,d_h}{kt_{nf}}\int_0^x\frac{dx}{T_w(x)-T_b(x)} \quad (12)$$

$$\mathrm{Re}=\frac{\rho_{nf}\,u_m\,d_h}{\mu_{bf}} \quad (13)$$

$$f=\frac{2\Delta P\,d_h}{L\,\rho_{nf}\,u_m{}^2} \quad (14)$$

The assessment of enhancement of heat transfer by using corrugated tubes and nanofluids and the penalty of pressure drop was performed by introducing performance evaluation criteria (*PEC*), which can be expressed as

$$PEC=\frac{(Nu/Nu_s)}{(f/f_s)^{1/3}} \quad (15)$$

The subscript *s* refers to smooth tubes.

3. Numerical Procedure and Validation

The solution of governing equations under prescribed boundary conditions was performed by using ANSYS/FLUENT 16. A nonuniform fine mesh was adopted near the wall due to the significance of velocity and temperature gradients, and the governing equations of momentum and energy were solved by adopting a second order upwind scheme. The SIMPLE algorithm was used to obtain a solution for the pressure-velocity coupling equation, and the PRESTO scheme was applied for the pressure correction equation. The residuals resulted from iterative solutions for the momentum and energy components are determined as 10^{-6} and 10^{-8}, respectively. A grid independence test of the

computational solution was carried out and 175,600 nodes in the mesh was found to be sufficient for solution accuracy and computational-time saving. For the sake of validation, the predicted friction factor of the present work was compared with that of the experimental findings of San and Huang [13] for flow in a corrugated tube as presented in figure 2a. Good agreement was found between the results of these works. In addition, the numerical code was validated by comparing the simulated results of the Nusselt number with those obtained by using the well-known Gnielinski correlation [14] of turbulent flow inside smooth tubes, as presented in Equation 16:

$$Nu = \frac{(f/8)(\mathrm{Re}-1000)\,\mathrm{Pr}}{1.07+12.7(f/8)^{1/2}(\mathrm{Pr}^{2/3}-1)}, \quad 3000 < \mathrm{Re} < 5\times10^{6}, \quad 0.5 < \mathrm{Pr} < 2000 \tag{16}$$

Reasonable agreement was shown between two results, as depicted in figure 2b.

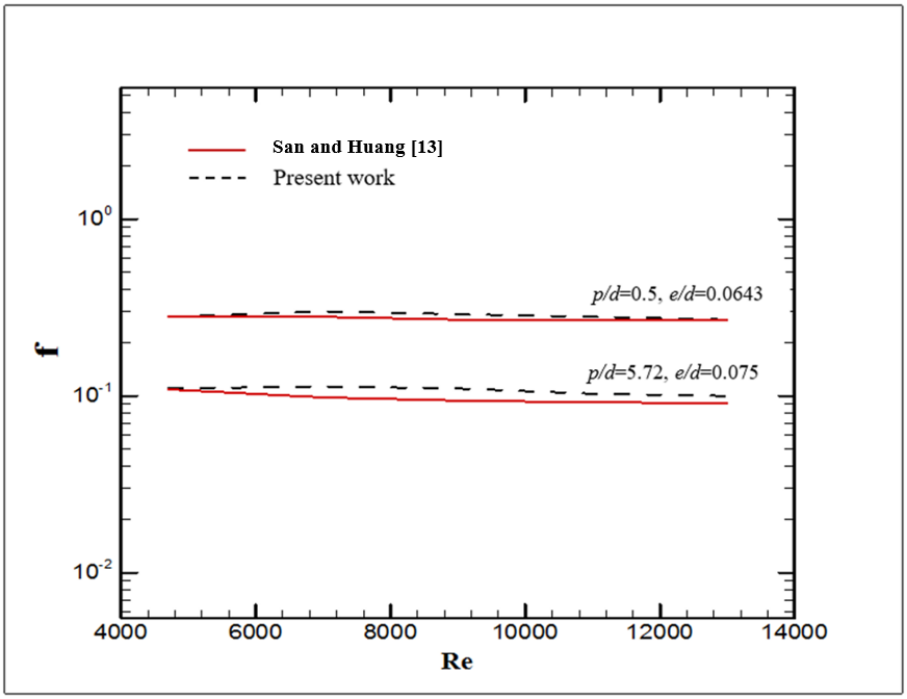

Figure 2a. Comparison of the simulated results for friction factor with those from San and Huang [13].

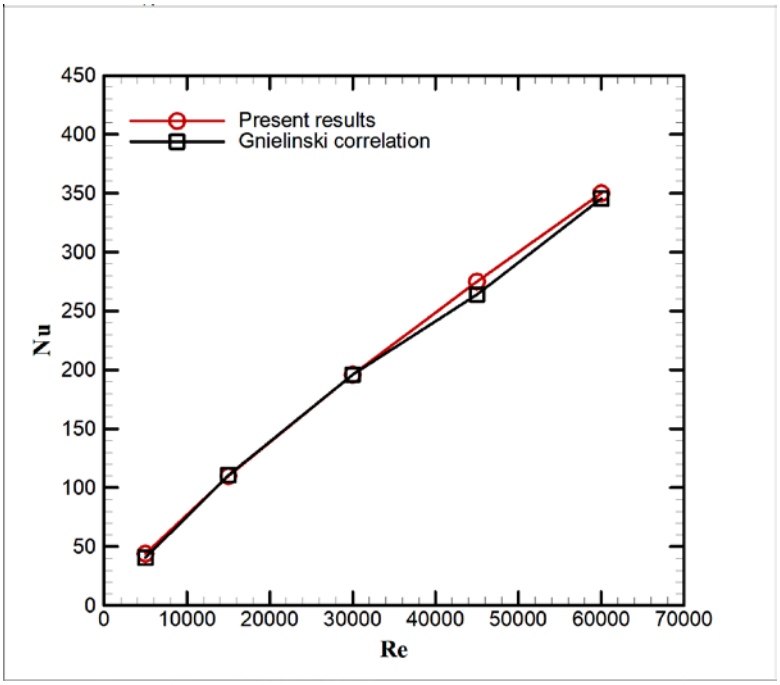

Figure 2b. Comparison of simulated results of the Nusselt number with those of the Gnielinski correlation [14].

4. Results and Discussion

The thermal and flow characteristics of the flow of SiO_2-water nanofluid in a corrugated tube were reported in terms of the average Nusselt number and friction factor as a function of nanoparticle volume concentration (0 to 4 vol.%) and nanoparticle diameter (30 to 80 nm) for a range of Reynolds numbers from 5,000 to 60,000.

The effects of dispersion of 30 nm diameter SiO_2 nanoparticles in water for various loadings on the rate of heat transfer as assessed by the Nusselt number are presented in figure 3. The rate of heat exchange clearly increases with the amount of nanoparticle dispersion. As the volumetric loading of nanoparticles increases, the effective thermal conductivity of nanofluids is enhanced, causing more conductive heat to be transferred, which in turn increases the heat transferred by convection. The irregular and random motion of the nanoparticles promotes greater momentum and energy transport throughout the nanofluid, and consequently, additional augmentation of heat transfer occurs. For comparison, the maximum enhancement of heat transfer in a dispersion of 4 vol.% of nanoparticles is approximately 16% larger than that seen in pure water at a Reynolds number of 60,000. The friction factor caused by using SiO_2-water nanofluids of various loadings of nanoparticles is depicted in figure 4. The friction factor of flow of the base fluid decreases with the increase of the Reynolds number due to the reduction in the thickness of the laminar sublayer. There is also a weak-dependence of the friction factor of nanofluids on the Reynolds number. This behaviour has been interpreted as the friction factor decreasing generally with the Reynolds number, while increasing with increments in the viscosity of nanofluids due to the dispersion of nanoparticles. Furthermore, as the loadings of nanoparticles increase, the pressure drops and the associated friction factor and required pumping

power is also increased. At the maximum Reynolds number, the maximum increase of friction factor due to using 4 vol.% nanofluid is about 5 times the factor seen in the base fluid.

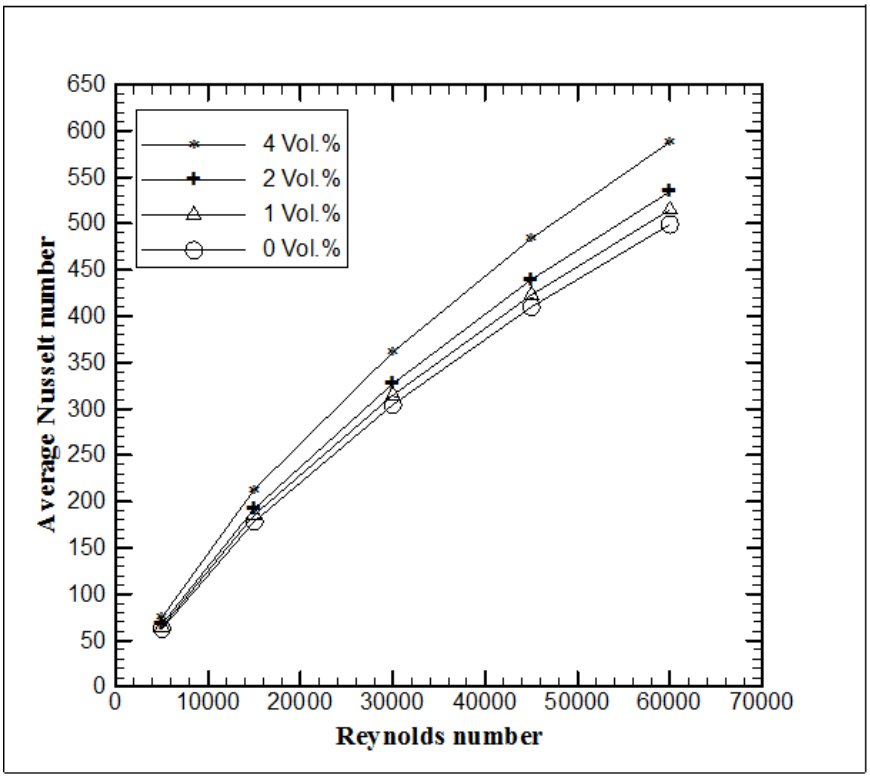

Figure 3. Nusselt number versus Reynolds number for different volumetric concentrations of nanoparticles of diameter 30 nm.

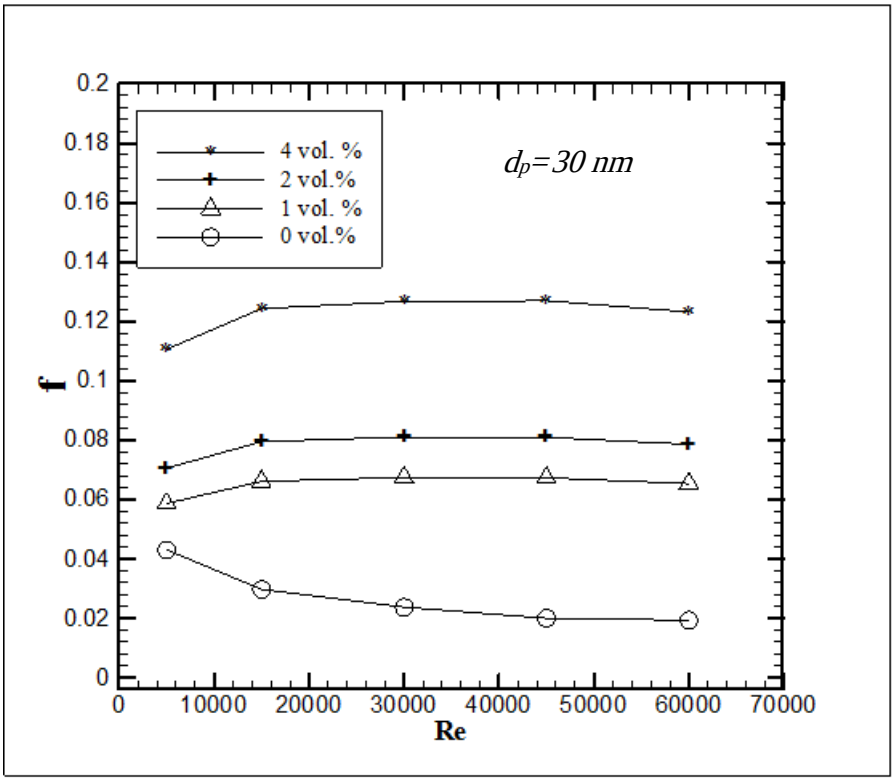

Figure 4. Friction factor for various Reynolds numbers and different volumetric loadings of nanoparticles of diameter 30 nm.

The effect of nanoparticle diameter ranging from 30 to 80 nm on the Nusselt number at 4 vol.% nanoparticle loading is presented in figure 5. It is clear that the dispersion of small-diameter nanoparticles leads to an enhancement of the Nusselt number. For the same volumetric loading of nanoparticles, small nanoparticles offer a higher surface contact area with the base fluid, which results in a considerable enhancement in thermal conductivity and a substantial increase in convective heat transfer coefficient. Therefore, the rate of heat exchange and the associated Nusselt number is increased. However, the effect of nanoparticle size on the rate of heat transfer seems to be generally insignificant. Only a 7.2% enhancement in heat transfer was observed when utilising 30 nm nanoparticles over a dispersion of 80 nm particles. The effect of the diameter of SiO_2 nanoparticles on the imposed friction factor for 4 vol.% nanofluids is illustrated in figure 6, and this appears to vary inversely with nanoparticle size. A reduction the size of nanoparticles for the same volumetric concentration increases the number of nanoparticles and surface contact area, which in turn result in an increase in viscosity and more friction and flow impedance being introduced. A dispersion of 30 nm-diameter nanoparticles exhibits a friction factor about 29% greater than that of 80 nm nanoparticles for 4. vol.%.

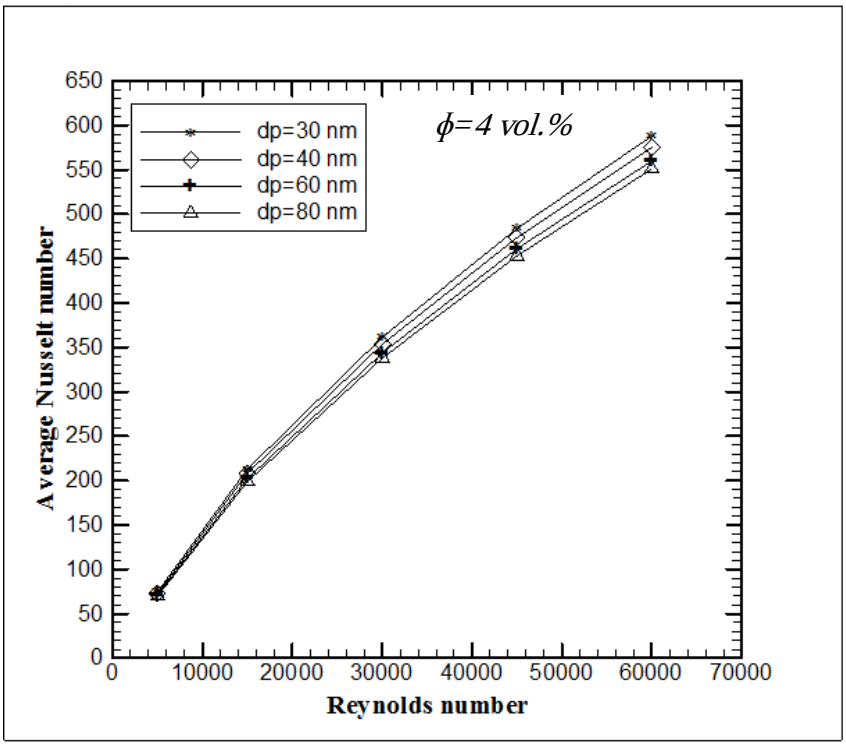

Figure 5. The effect of nanoparticle size on the Nusselt number at ϕ=4 *vol.*%.

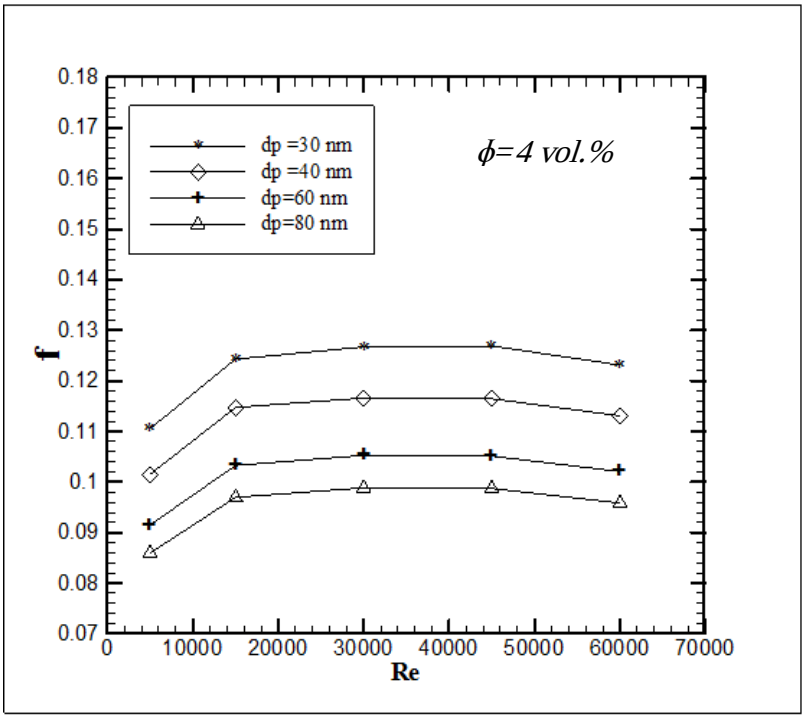

Figure 6. The effect of nanoparticle size on the friction factor at ϕ=4 *vol.*%.

The combined effect of applying two techniques of heat transfer enhancement (a roughness element in the form of corrugation and the dispersion nanoparticles at 4 vol.% and d_p=30 nm) on the performance evaluation criteria is presented in figure 7. At the lower Reynolds numbers, the enhancement in heat transfer was higher than the penalty caused by the introduced pressure drop, leading to a higher PEC. As the Reynolds number increased, the increase in viscosity and associated pressure drop and friction factor of nanofluids in the corrugated tube caused a monotonic reduction in the PEC. At Re≥ 40,000, the performance of the flowing nanofluid in the corrugated tube deteriorated to below that of the water in the smooth tube as the higher friction factor penalty exceeded the augmentation in heat transfer.

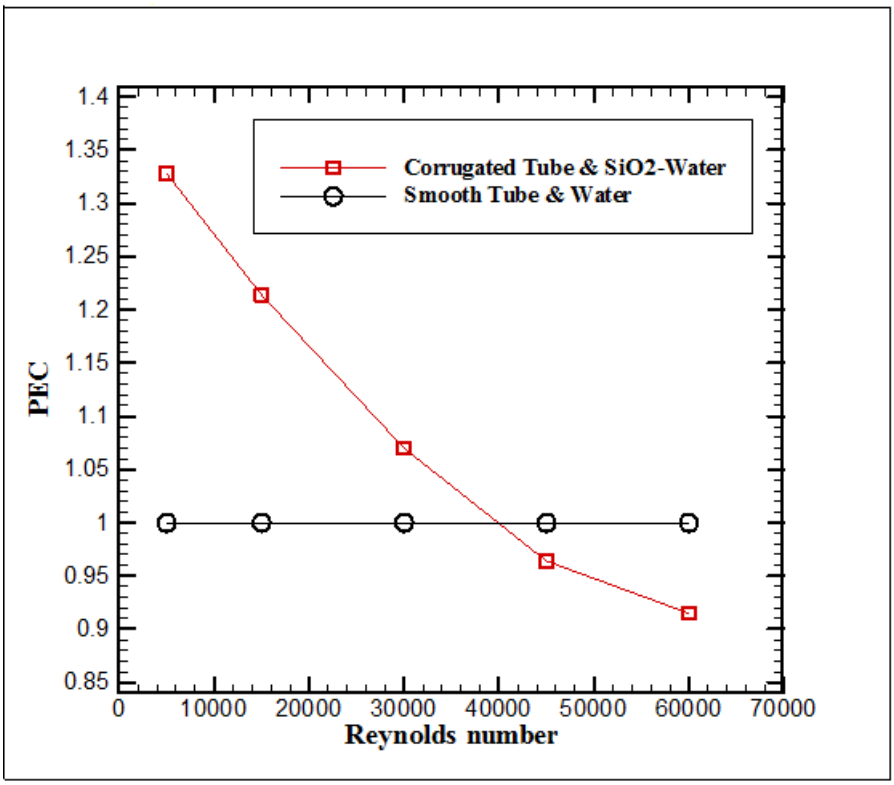

Figure 7. Variation of performance evaluation criteria with Reynolds number.

5. Conclusions

Simulation of turbulent forced convection flow of SiO2-water nanofluids in a corrugated tube was performed so that the effects of the Reynolds number and both volumetric concentration and diameter of nanoparticles on thermal and hydrodynamic performance could be examined. It can be inferred that dispersion of nanoparticles in the base fluid enhances thermal performance at the expense of a pressure drop. The rate of heat transfer and imposed pressure drop vary significantly with the concentration of nanoparticles, whereas the size of nanoparticles has a relatively inconsequential effect on the thermal and hydrodynamics characteristics. Additionally, the techniques of heat transfer enhancement (corrugation and nanoparticle dispersion) are only effective at values of Reynolds number <40,000.

References

[1] Lee S, Choi S, Li S and Eastman J 1999 Measuring Thermal Conductivity of Fluid Containing Oxide Nanoparticles *Transactions of the ASME, Journal of Heat Transfer* **121** pp 280-9

[2] Darzi A R, Farhadi M, Sedighi K, Shafaghat R and Zabihi K 2012 Experimental investigation of turbulent heat transfer and flow characteristics of SiO2/water nanofluid within helically corrugated tubes *International Communications in Heat and Mass Transfer* **39** pp 1425–34.

[3] Manca O, Nardini S and Ricci D 2012 A numerical study of nanofluid forced convection in ribbed channels *Applied Thermal Engineering* **37** pp 280–92

[4] Darzi A R, Farhadi M, Sedighi K, Aallahyari S and Delavar M A 2013 Turbulent heat transfer of Al2O3–water nanofluid inside helically corrugated tubes: Numerical study *International Communications in Heat and Mass Transfer* **41** pp 68–75

[5] Darzi A R, Farhadi M and Sedighi K 2014 Experimental investigation of convective heat transfer and friction factor of Al_2O_3/water nanofluid in helically corrugated tube *Experimental Thermal and Fluid Science* **57** pp 188–99

[6] Al-Shamani A N, Sopian K, Mohammed H A, Mat S, Ruslan M H and Abed A M 2015 Enhancement heat transfer characteristic in the channel with Trapezoidal rib–groove using nanofluids *Case Studies in Thermal Engineering* **5** pp 48–58

[7] Khdher A M, Sidik N C, Mamat R and Hamzah W W 2015 Experimental and numerical study of thermo-hydraulic performance of circumferentially ribbed tube with Al_2O_3 nanofluid *International Communications in Heat and Mass Transfer* **69** pp 34–40

[8] Navaei A S, Mohammed H A, Munisamy K M, Yarmand, H and Gharehkhani S 2015 Heat transfer enhancement of turbulent nanofluid flow over various types of internally corrugated channels *Powder Technology* **286** pp 332–41

[9] Yang D, Sun B, Li H and Fan X 2015 Experimental study on the heat transfer and flow characteristics of nanorefrigerants inside a corrugated tube *International Journal of Refrigeration* **56** pp 213–23

[10] Andreozzi A, Manca O, Nardini S and Ricci D 2016 Forced convection enhancement in channels with transversal ribs and nanofluids *Applied Thermal Engineering* **98** pp 1044–53

[11] Kumar S, Kothiyal A D, Bisht M S and Kumar A 2017 Turbulent heat transfer and nanofluid flow in a protruded ribbed square passage *Results in Physics* **7** pp 3603–18

[12] Qi C, Wan Y, Li C, Han D and Rao Z 2017 Experimental and numerical research on the flow and heat transfer characteristics of TiO_2-water nanofluids in a corrugated tube *International Journal of Heat and Mass Transfer* **115** pp 1072–84

[13] San J Y and Huang W C 2006 Heat transfer enhancement of transverse ribs in circular tubes with consideration of entrance effect *International Journal of Heat and Mass Transfer* **49** pp 2965–71

[14] Gnielinski V 1976 New equations for heat and mass transfer in turbulent pipe and channel flow *International Chemical Engineering* **16** pp 359–368